Characterization of crystallization pathways during cholesterol precipitation from human gallbladder biles: identical pathways to corresponding model biles with three predominating sequences[1]

David Q-H. Wang and Martin C. Carey[2]

Department of Medicine, Gastroenterology Division, Brigham and Women's Hospital, Harvard Medical School and Harvard Digestive Diseases Center, 75 Francis Street, Boston, MA 02115

Abstract In model biles, five crystallization sequences are present as functions of bile salt/lecithin (egg yolk) ratio and their positions on phase diagrams are influenced by bile salt hydrophobicity, temperature, and total lipid concentration (D. Q-H. Wang and M. C. Carey. *J. Lipid Res.* 1996.**37**: 606–630). To determine whether the same pathways occur ex vivo during cholesterol precipitation from human gallbladder biles, we examined 22 cholesterol gallstone (CSI = 1.56 ± 0.26), 4 pigment gallstone (0.69 ± 0.06), and 4 control biles (0.85 ± 0.22) by microscopy and lipid analytic techniques for 30 days. Temperature was varied (4–45°C) to move relative compositions into adjacent pathways or supersaturated zones to test whether the same bile could be forced to crystallize in different sequences. Sequences in native bile were identical to those in model systems composed of mixed bile salts–lecithin–cholesterol mixtures, and three corresponding pathways (***B, C, D;*** op. cit.) were observed at 37°C. With increasing lecithin content, we found *i*) ***B:*** plate-like cholesterol monohydrate crystals appeared before arc-shaped (putatively anhydrous cholesterol) crystals which transformed via helices and tubules into plate-like crystals and no liquid crystals formed; *ii*) ***C:*** lamellar liquid crystals, typified by birefringent multilamellar vesicles, were detected before cholesterol monohydrate crystals, and subsequently arc, helical and tubular crystals appeared; and *iii*) ***D:*** precipitation of lamellar liquid crystals was followed by cholesterol monohydrate crystals and no arc crystals were detected. Added EDTA prevented calcium bilirubinate formation, but crystallization sequences in these biles were identical to those without EDTA. We conclude that *i*) cholesterol crystallization pathways and sequences in human gallbladder biles are identical to model biles matched for appropriate physical-chemical conditions; *ii*) three of the five sequences observed in model biles were found in native bile; and *iii*) calcium bilirubinates neither promote biliary cholesterol crystallization nor influence crystal growth.—**Wang, D. Q-H., and M.C. Carey.** Characterization of crystallization pathways during cholesterol precipitation from human gallbladder biles: identical pathways to corresponding model biles with three sequences predominating. *J. Lipid Res.* 1996. **37:** 2539–2549.

Supplementary key words gallstones • microscopy • bile salts • phospholipid • phase diagrams • chelation • calcium • bilirubinate

Rapid ex vivo precipitation of cholesterol monohydrate (ChM) crystals from the "isotropic phase" of gallbladder bile discriminates cholesterol (Ch) gallstone biles from supersaturated biles of controls (1). Despite extensive work aimed at identifying factors influencing ChM crystal detection times in bile (2), little attention has been paid to the possibility that different Ch crystallization sequences could occur in native biles. Konikoff et al. (3) highlighted this lack of information when they found a new Ch crystallization pathway in a dilute taurocholate-containing model bile that differed radically from the liquid crystal to solid ChM crystal pathway first described by Holzbach and Corbusier (4). In a recent systematic survey of Ch crystallization from model bile (5), we observed five crystallization pathways with stepwise increases in bile salt (BS) to lecithin (L) ratio, each displaying a different set of crystallization sequences. Positions of the pathways on phase diagrams were shown to be influenced by temperature, BS hydrophobicity, and total lipid concentration [TL] (5). Although calcium is present in substantial concentrations in bile (6) and often precipitates as inorganic and organic salts in gallstones (7–9), we found that even superphysiological (5–20 mM) levels of added calcium did not influence crystal detection times nor micellar Ch solubility in model biles but were a strong crystal growth agent (5) especially at the higher concentrations.

Abbreviations: BS, bile salt; Ch, cholesterol; ChM, cholesterol monohydrate; CSI, cholesterol saturation index; HPLC, high performance liquid chromatography; L, lecithin; MBS, mixed bile salts; [TL], total lipid concentration.

[1]This paper was presented in part at the 1995 Annual Meeting of the American Gastroenterological Association, San Diego, CA and published as an abstract in *Gastroenterology.* 1995. **108:** A1196.

[2]To whom correspondence should be addressed.

The present study was designed to investigate how crystallization pathways in human bile correlate with those of matched model biles, and to examine effects of calcium on Ch crystallization rates by using a chelation strategy. We classified sterile human biles according to the Ch content of the stones and then examined the ultracentrifuged and microfiltered biles microscopically for 30 days at four temperatures. Native Ch crystallization pathways were found to be identical to those in matched model systems (5) with three pathways predominating at 37°C. The strategy of incubating the same bile at different temperatures showed that bile could crystallize in several sequences depending on the ambient physical–chemical conditions. This systematic study provides a framework for further investigation of the effects of endogenous and exogenous pro- and anti-crystallizing factors on Ch crystallization from native bile.

METHODS

Chemicals

The disodium salt of ethylenediaminetetraacetate (EDTA) was obtained from Fisher Scientific Co. (Fair Lawn, NJ). For HPLC analyses of BS molecular species, all reagents were HPLC grade and were purchased from Fisher Scientific Co. (Medford, MA). Other chemicals and solvents were American Chemical Society (ACS) or reagent grade quality (Fisher Scientific Co.) and identical to those used in our previous work (5).

Gallbladder biles: collection and preparation

Fresh gallbladder biles, together with one representative gallstone from each gallbladder, were collected at elective laparoscopic cholecystectomy under a protocol approved by the Institutional (BWH) Human Subjects Committee and written informed consent was obtained. All patients had normal liver function tests and functioning gallbladders by ultrasonography and no historical, clinical, or laboratory evidence of present or prior hepatobiliary infection or other complications. As defined by gallstone analysis (see below), 22 gallbladder biles were collected from patients with Ch gallstones, 4 from patients with pigment gallstones, and 4 from controls who did not have evidence of stones or biliary sludge at the time of surgery. A small portion of each bile sample was cultured to exclude aerobic and anaerobic infection.

Biles were aspirated with a large-bore hypodermic needle and syringe at the beginning of the operative procedure prior to gallbladder manipulation, retraction, clamping, or dissection of Calot's triangle. In general, only gallbladders that provided at least 12 ml of bile and complete gallbladder emptying were entered in the study. After dividing the bile samples into two equal portions, one aliquot was added to sterile glass tubes containing an EDTA concentration sufficient to bind typical physiological levels of biliary calcium (10). Test tubes were prepared by drying a 1-ml aqueous film of 60 mM EDTA so that the final EDTA concentration was ≈10 mM in 6 ml bile. The pH was checked by a Standard pHM82 pH Meter (Radiometer, Copenhagen) and, when found to be somewhat lower with EDTA, was adjusted to within 0.1 pH unit of the other portion with 20–50 μl 1 M NaOH. After both tubes were ultracentrifuged at 100,000 *g* for 30 min at 37°C, the sediments were examined by direct and polarizing light microscopy. Mucus gel was observed microscopically as nonbirefringent amorphous strands and verified by periodic acid/Schiff (PAS) staining (11). To ensure further clarification, samples were then filtered through a preheated (37°C) Swinnex-GS filter assembly containing a 0.22-μm filter (Millipore Products Division, Bedford, MA) to remove mucus gel and to generate a bile specimen containing no solid/liquid crystals or other particulate matter when observed by polarizing light microscopy (magnification × 400).

Detection of Ch crystals, liquid crystals, and phase transitions

Gallbladder biles with and without EDTA were divided equally into two sets of 4 tubes each. The tubes were flushed with N_2, sealed with Teflon-lined caps, and incubated individually at 4°C, 23°C, 37°C, and 45°C. Detection of Ch crystals, liquid crystal, and phase transitions as well as crystallization sequences was performed by polarizing light microscopy at × 400 magnification (5). ChM crystals and aggregated liquid crystals were recorded by 35 mm time-lapse photography within the first 5 days of Ch crystallization studies. Processed films were used for size measurement of crystals and liquid crystals. Sizes of ChM crystals were estimated by assuming the crystal area of a parallelogram. Sizes of aggregated liquid crystals were estimated by using approximate diameters of the surface areas.

Chemical analyses

Small portions of the original biles with and without EDTA were stored at −20°C for lipid analysis followed by ultracentrifugation and microfiltration. After 30 days of incubation, all biles were passed through preheated (37°C) Swinnex-GS 0.22-μm filters and then reanalyzed for relative and absolute lipid compositions. Total BS were quantified by the 3α-hydroxysteroid dehydrogenase method (12), L by the inorganic phosphorus pro-

cedure (13), and Ch enzymatically (14). CSIs of native biles were calculated from critical tables (15). Gallstones were washed with distilled water, dried at room temperature, ground to a powder in an agate mortar, and dissolved in isopropanol. Ch content of gallstones (wt/wt) was measured enzymatically (14) and by HPLC (16). Stones with a Ch content of >80% or <20% by weight were classified as Ch or pigment gallstones, respectively. Conjugated BS compositions were determined by the HPLC method of Rossi, Converse, and Hofmann (17) and total calcium concentration was determined by atomic absorption spectrometry (18) using Perkin-Elmer models 4100ZL and 2280 (Perkin-Elmer Corp., Norwalk, CT).

Statistical methods

Data are expressed as means ± SD. Statistically significant differences between values for Ch stone patients, pigment stone patients, and healthy controls, and between bile samples either with or without EDTA were assessed by Student's *t*-test. Statistical significance was defined as a two-tailed probability of less than 0.05.

RESULTS

Lipid compositions, microscopic studies, and crystallization pathways

Table 1 lists individual and mean bile compositions before and after 30 days equilibration. Of note is that with EDTA, mean compositions prior to crystallization were within 0.2% of the non-EDTA samples. Furthermore, at equilibrium CSIs (mean = 0.99) of cholesterol gallstone biles were significantly ($P < 0.0001$) smaller than original values, whereas CSI values of pigment and control biles were not statistically different from initial analyses after 30 days. **Figure 1** plots the relative lipid compositions of gallbladder biles before and after 30 days on a mixed BS (MBS)–L–Ch phase diagram (5) (pH 7.0, 37°C, 0.15 M NaCl). We used an extrapolated mean [TL] value of ≈ 11 g/dL for the limits of the micellar zone despite the fact that the [TL] range was 4 to 24 g/dL (Table 1). Figure 1 also depicts regions ***A***, ***B***, ***C***, ***D***, and ***E*** from our model bile study (5) that indicate pathways with five distinct Ch crystallization sequences (5). It is apparent that all Ch gallstone biles plotted in regions ***B***, ***C***, and ***D***, with most in regions ***B*** and ***C***. At equilibrium all relative biliary compositions plotted on or close to the micellar phase limits although considerable variation was present because of the [TL] range (see above and Table 1). All pigment stone and control biles plotted within the micellar zone of the phase diagram (Fig. 1).

Before centrifugation and filtration, ChM crystals and mucus gel were observed microscopically in all biles from patients with Ch gallstones. Mucus gel was further confirmed by PAS staining (11). Moreover, non-birefringent liquid crystals were also observed, but only in biles that plotted in regions ***C*** and ***D*** (Fig. 1), as was expected for these compositions (5). Tubular crystals (3) were found in two of eight fresh biles whose lipid compositions plotted in region ***B*** (Fig. 1). In no gallbladder bile from patients with pigment gallstones or controls were either solid Ch crystals, liquid crystals, or mucus gel observed. After centrifugation and filtration at 37°C, no crystalline precipitates or mucus gel were visualized microscopically and the biles were considered isotropic.

Habits of solid Ch crystals and liquid crystals observed were essentially identical to those described in our earlier work on model bile (5). **Figure 2** shows representative photomicrographs of a transitional sequence between less well known crystal habits in human bile. Arc-like crystals (Fig. 2a) were short curved rods. After a few days, they elongated and coiled into right-handed regular helices (Fig. 2b). Over time, helical crystals (Fig. 2c) became wider with pitch angles of 56° that progressively decreased to 11° (5, 19). Finally, helices fused to form ribbed cylindrical tubular crystals (Fig. 2d) that usually fractured at their ends (Fig. 2d) to produce plate-like ChM crystals with angles of 79.2° and 100.8°, and often a notched corner (5). Of note is that for the same time points, sizes of ChM crystals (n = 160) were significantly larger (216.8 ± 223.4 μm^2/per ChM plate) in human gallbladder biles ($P < 0.0001$) than in model bile systems (84.0 ± 71.4 μm^2/per ChM plate). Filamentous crystals (3) believed to be analogous to arc-like crystals (5) were detected during crystallization at 23° and 37°C in only two bile samples whose lipid compositions plotted in region ***B*** (Fig. 1). For all biles plotting in region ***B***, ChM crystals appeared in about 2–4 days followed by transient arcs, helical, and tubular crystals (Fig. 2). In region ***C***, small, aggregated, and fused liquid crystals (5) preceded appearance of ChM crystals, and were followed by arc, helical, and tubular crystals (Fig. 2). In region ***D***, small, aggregated, and fused liquid crystals preceded solid ChM crystals but no anhydrous Ch crystals appeared.

Effects of temperature on biliary Ch crystallization

By using the strategy of incubating the same bile at different temperatures, we allowed crystallization pathways to vary without perturbing the concentration of any solute in bile: in particular, total and relative lipid compositions remained constant (**Fig. 3**). With bile no.

TABLE 1. Analytical lipid compositions of gallbladder biles

No	Day 0					30 Days				
	Mole%BS	Mole%L	Mole%CH	[TL]	CSI[a]	Mole%BS	Mole%L	Mole%CH	[TL]	CSI[a]
				g/dl					*g/dl*	
Cholesterol gallstones										
1	65.94	21.41	12.65	11.30	1.69	73.72	19.82	6.46	10.36	0.97
2	66.98	21.89	11.13	23.24	1.33	72.86	19.58	7.56	21.78	0.99
3	61.32	24.91	13.77	24.20	1.54	71.02	21.00	7.98	20.13	0.95
4	69.16	21.33	9.51	7.90	1.41	76.32	17.94	5.74	6.45	1.00
5	75.79	16.35	7.86	14.91	1.22	79.84	14.45	5.71	12.68	1.00
6	67.70	21.77	10.53	4.14	1.67	72.31	21.60	6.09	3.98	1.01
7	72.34	19.71	7.95	12.89	1.12	76.24	17.53	6.23	11.79	0.98
8	71.30	21.14	7.56	9.02	1.09	76.83	17.34	5.83	8.13	0.99
9	69.18	18.50	12.32	9.81	1.86	77.18	16.95	5.87	8.41	1.01
10	73.56	18.37	8.06	8.61	1.29	79.85	14.93	5.22	7.82	0.99
11	66.82	19.73	13.45	10.69	1.89	75.72	18.11	6.17	9.13	0.99
12	69.15	19.29	11.56	11.48	1.64	78.82	15.59	5.59	10.82	0.97
13	65.92	20.98	13.10	8.47	1.86	73.12	20.35	6.53	7.65	1.00
14	69.33	21.17	9.50	14.62	1.26	74.26	18.91	6.83	12.89	0.99
15	77.24	12.50	10.26	13.47	1.91	84.24	11.13	4.62	11.81	1.02
16	57.25	27.56	15.19	17.80	1.68	69.83	22.36	7.81	14.61	1.01
17	64.28	22.88	12.84	18.58	1.51	72.39	20.17	7.44	16.26	1.00
18	78.57	13.82	7.62	8.97	1.47	82.74	12.77	4.49	7.13	0.95
19	66.21	22.42	11.37	11.24	1.49	73.70	19.55	6.75	9.91	1.02
20	61.04	24.35	14.61	8.42	1.91	71.14	22.25	6.61	6.58	0.99
21	72.35	16.89	10.76	10.53	1.71	78.36	16.20	5.44	8.81	0.97
22	70.85	18.99	10.16	5.77	1.69	78.31	16.64	5.05	4.80	0.98
Mean	68.74 ± 5.24	20.27 ± 3.46	10.99 ± 2.33	12.09 ± 5.13	1.56 ± 0.26	75.85 ± 3.83	17.96 ± 2.99	6.18 ± 0.96	10.54 ± 4.54	0.99 ± 0.02
Mean (EDTA)	68.86 ± 3.72	20.50 ± 2.09	10.64 ± 2.26	12.15 ± 5.44	1.49 ± 0.28					
Pigment gallstones										
23	79.51	16.57	3.92	5.73	0.76	81.26	15.56	3.18	5.21	0.65
24	72.25	22.73	5.02	9.94	0.69	71.42	24.20	4.38	8.43	0.61
25	65.95	28.67	5.38	7.42	0.70	67.21	28.66	4.13	6.86	0.55
26	71.51	24.23	4.26	7.54	0.61	72.63	23.45	3.92	6.97	0.57
Mean	72.31 ± 5.57	23.05 ± 5.00	4.65 ± 0.67	7.66 ± 1.73	0.69 ± 0.06	73.13 ± 5.90	22.97 ± 5.45	3.90 ± 0.52	6.87 ± 1.32	0.60 ± 0.04
Mean (EDTA)	71.96 ± 6.35	23.42 ± 5.75	4.63 ± 0.67	7.73 ± 1.95	0.69 ± 0.08					
Control biles without stones										
27	68.49	26.42	5.09	16.72	0.60	68.64	27.58	3.78	13.92	0.46
28	77.07	16.93	6.01	8.81	1.03	82.57	12.80	4.63	7.82	0.98
29	60.14	31.99	7.86	5.66	1.04	64.87	27.87	7.26	5.26	1.00
30	69.98	24.96	5.06	5.95	0.73	74.21	21.77	4.02	5.17	0.65
Mean	68.92 ± 6.95	25.08 ± 6.22	6.01 ± 1.31	9.29 ± 5.16	0.85 ± 0.22	72.57 ± 7.69	22.51 ± 7.05	4.92 ± 1.60	8.04 ± 4.11	0.77 ± 0.26
Mean (EDTA)	68.64 ± 6.88	25.37 ± 6.19	5.99 ± 1.38	9.01 ± 4.73	0.85 ± 0.22					

Abbreviations: Ch, cholesterol; L, egg yolk lecithin; BS, bile salts; [TL], total lipid concentration; CSI, cholesterol saturation index.
[a]CSI is calculated according to the critical tables (15).

7 (Table 1) whose relative lipid composition plotted in region ***B*** at 37°C (left panels of Fig. 3a), ChM crystals appeared first, followed by arc, helical, and tubular crystals, but no liquid crystals appeared (right panel of Fig. 3a). At 23°C, phase boundary ***ab*** moved to the left (5), and forced the lipid composition to plot in region ***C*** (Fig. 3a). As shown on the right panel (Fig. 3a), the crystallization sequence altered to that expected for region ***C*** (5); crystallization began with small, aggregated, and fused liquid crystals, followed by ChM crystals and then arc, helical, and tubular crystals. At 4°C (right panel of Fig. 3a), the lipid composition of the bile moved further into region ***C,*** and the crystallization sequence remained the same as at 23°C, but the precipitation events were delayed appreciably.

Figure 3b shows bile no. 1 (Table 1) whose relative lipid composition plotted in region ***C*** at 23° and 37°C. At these temperatures, small, aggregated, and fused liquid crystals appeared first, followed by ChM crystals and then arc, helical, and tubular crystals (right panel of Fig. 3b). Moreover, when the temperature was decreased to 4°C (left panel of Fig. 3b), the lipid composition plotted in region ***D,*** and the crystallization sequence changed to that expected for ***D*** (right panel of Fig. 3b), in that

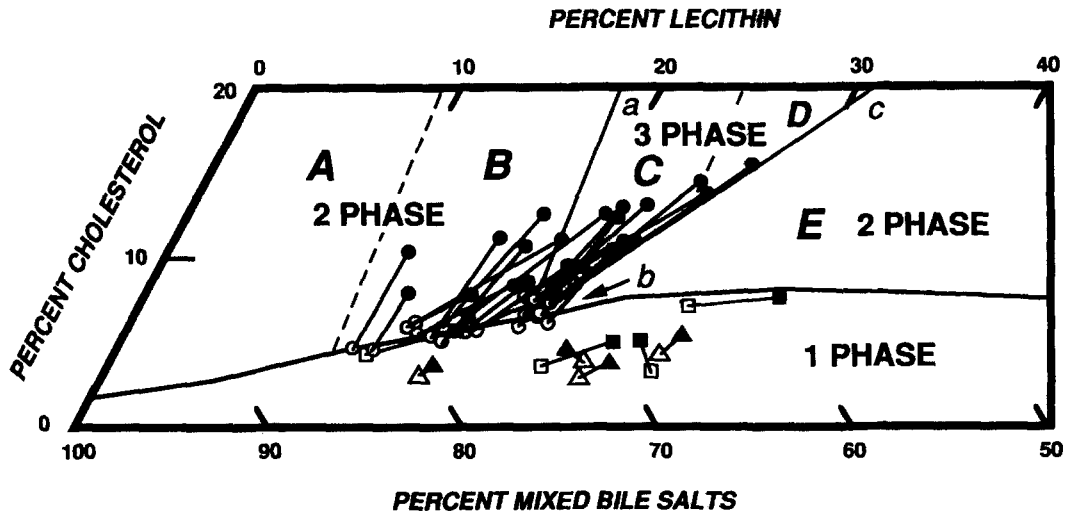

Fig. 1. Relative lipid compositions (moles per 100 moles) of gallbladder biles from patients with Ch and pigment gallstones as well as controls, plotted on a condensed phase diagram for the average total lipid concentration (≈ 11 g/dL) of the bile samples (Table 1). The MBS (mixed bile salts)–L (lecithin)–Ch (cholesterol) phase boundaries (pH 7.0, 0.15 M NaCl) were extrapolated at 37°C from ref. 5 as were the phase limits of the micellar zone. The one-phase micellar zone is enclosed by the solid line at the bottom. Above the micellar zone, two solid lines (***ab*** and ***bc***) divide the two-phase zones from a central three-phase zone. Based upon the solid and liquid crystallization sequences present in model MBS–L–Ch systems (same conditions), the left two-phase and central three-phase regions are divided by dashed lines into regions ***A, B, C, D,*** and ***E***. Relative lipid compositions of gallbladder biles at beginning (closed symbols) and end (open symbols) of 30 days crystallization at an incubation temperature of 37°C. Symbols ● relative lipid composition of Ch gallstone biles, ▲ pigment gallstone biles, and ■ controls (no stones).

precipitation of small, aggregated, and fused liquid crystals preceded ChM crystallization.

Figure 3c displays bile no. 6 (Table 1) whose relative lipid composition plotted in region ***D*** at 37°C. Small, aggregated, and fused liquid crystals appeared before ChM crystals, but no arc, helical, or tubular crystals ever appeared (right panel of Fig. 3c). When the temperature was decreased to 23°C and 4°C, the lipid composition of the bile remained in region ***D*** (left panel of Fig. 3c). Although the crystallization pathway and sequence remained unaltered, ChM crystal detection times were delayed at the lower temperature (5).

Figure 3d shows that when the relative lipid composition of a normal bile (no. 30, Table 1) plotted in the micellar zone of the phase diagram at 37° and 23°C, no solid Ch crystals or liquid crystals were observed. However, because the micellar zone contracted at 4°C (5) and phase boundary ***ab*** moved to the left (left panel of Fig. 3d) the relative lipid composition of the bile entered region ***E***. As expected for crystallization in this region (5), precipitation of small, aggregated, and fused liquid crystals occurred, but no solid Ch crystals appeared.

In the case of all control and pigment gallstone micellar biles, no solid Ch or liquid crystals were ever detected at 37°C. At 23°C, only one control bile (no. 28) formed ChM crystals and then anhydrous Ch crystals, as its relative lipid composition entered region ***B*** during crystallization (5). Because phase boundary ***ab*** shifted to the left at 4°C, the relative lipid composition of the same bile entered region ***C*** altering the crystallization sequence to liquid crystals followed by ChM crystals and then anhydrous Ch crystals (5). Although the other control and pigment gallstone biles displayed liquid crystals at 4°C (Fig. 1), no solid crystals were ever produced consistent with the lipid compositions of model systems plotting in region ***E*** (5).

Average sizes of liquid crystals (n = 29) were appreciably larger (472.0 ± 361.8 μm^2/per aggregate) at 4°C than at 37°C (136.5 ± 263.1 μm^2/per aggregate) ($P < 0.01$), while sizes of solid crystals (n = 107) had the reverse trend being significantly larger (216.8 ± 223.4 μm^2/per ChM plate) at 37°C than at 4°C (40.4 ± 35.4 μm^2/per ChM plate) ($P < 0.0001$).

Relative lipid compositions of gallbladder biles after crystallization

As expected after the 30-day period, the CSI values of all Ch gallstone biles (Table 1) displayed highly significant changes reaching equilibrium (CSI approximately 1) in accordance with predictions of the critical tables (15). However, no significant changes occurred in any of the pigment stone or control biles. As noted in model systems (5), the relative lipid compositions during Ch crystallization did not follow lines of constant L to BS ratio, but demonstrated progressive decreases in L mole fraction (Fig. 1). Biles initially plotting in region ***B*** at 37°C (Fig. 1) remained in that pathway during

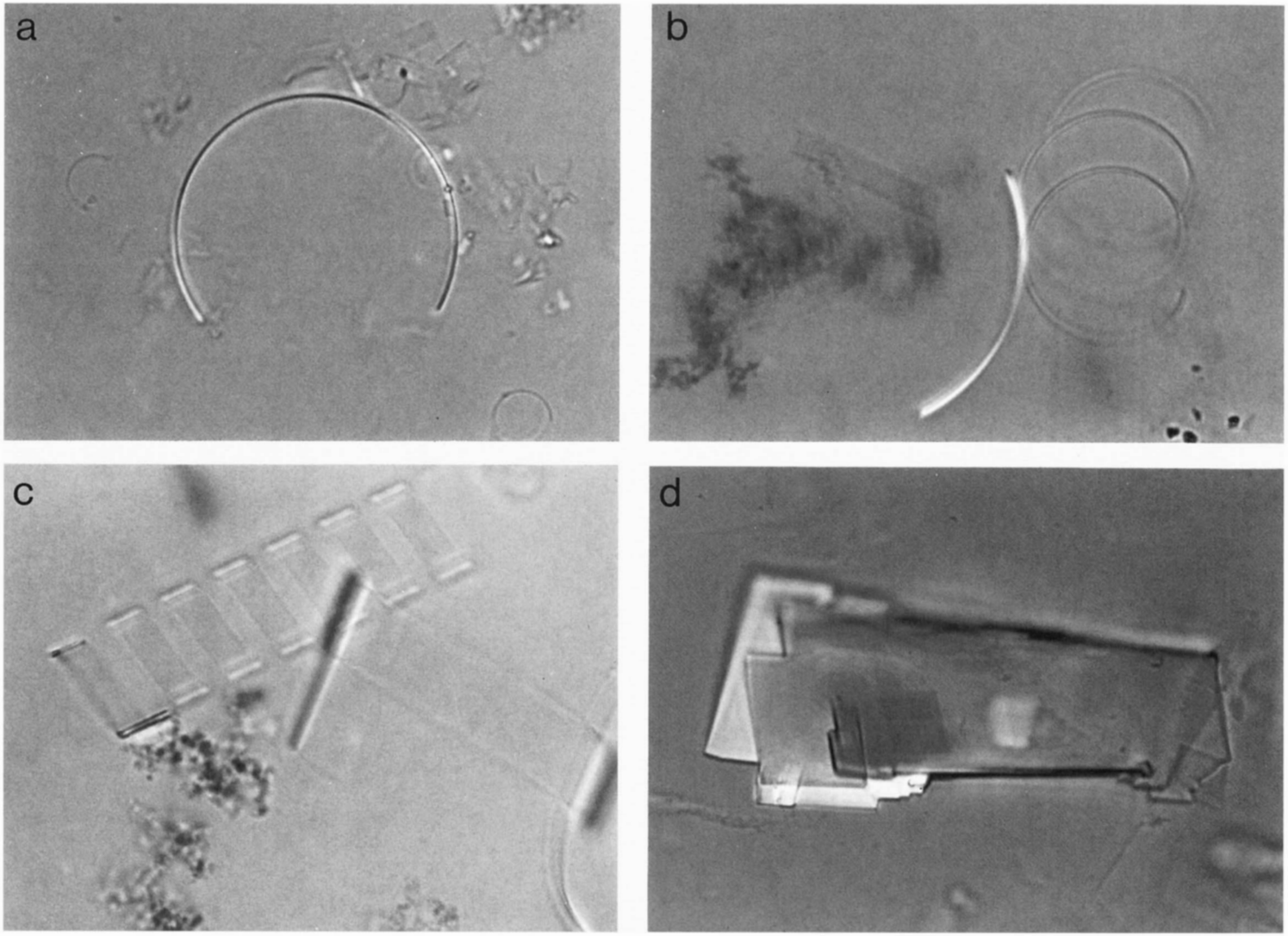

Fig. 2 Habits of solid Ch crystals observed by polarizing light microscopy in human Ch gallstone biles whose lipid compositions plotted in pathways B and C of Fig. 1. (a) Arc-like crystal. (b) A right-handed helical crystal together with rod-shaped and plate-like crystals. (c) Conversion of a helix to a tubular crystal. (d) Tube-like crystal fracturing at ends to produce plate-like ChM crystals, with 79.2° and 100.8° angles, and with a notched corner. (All magnifications × 800) (cf. ref. 5).

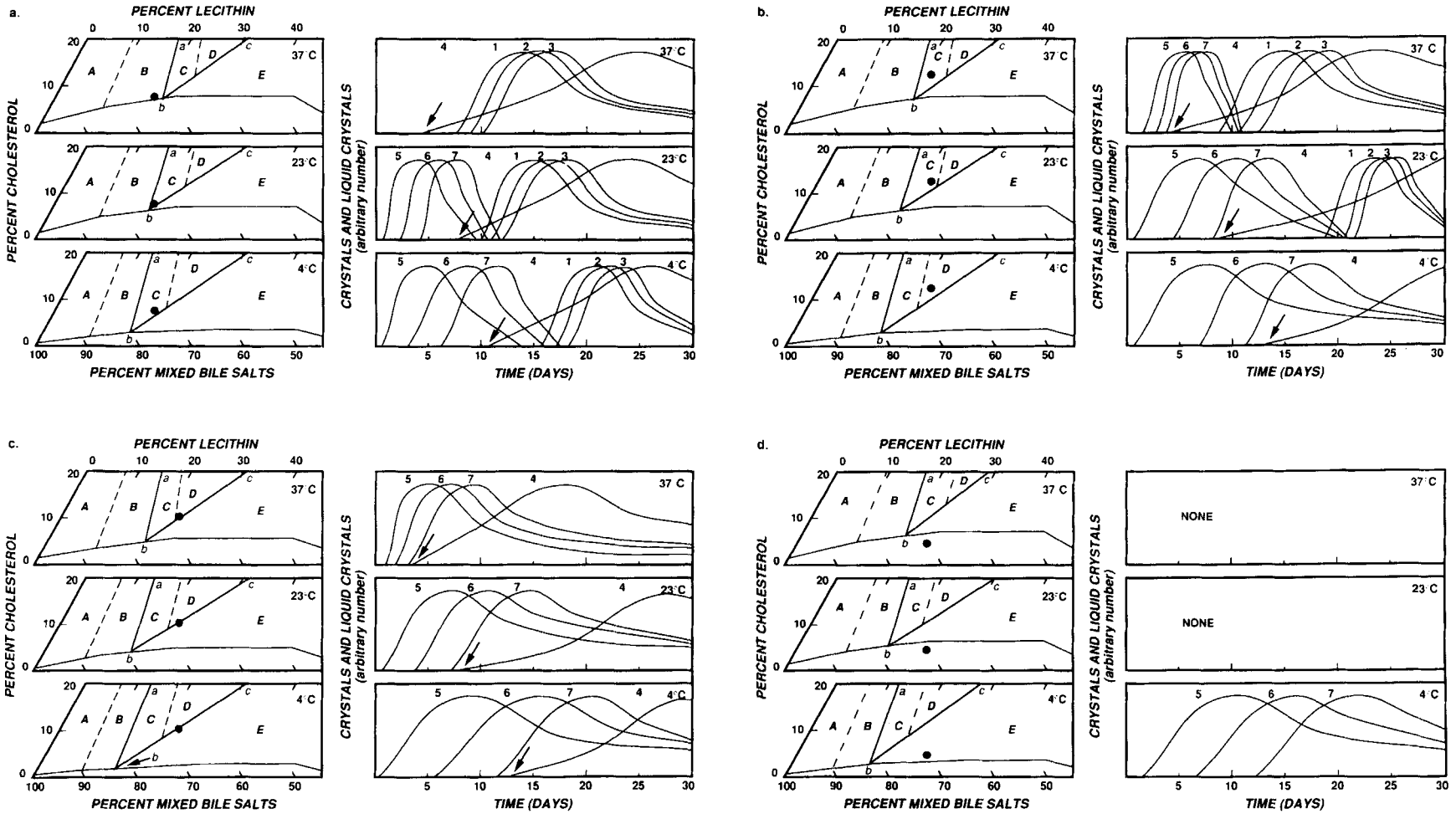

Fig. 3. Temperature dependence of the condensed phase diagram (left) and crystallization pathways (right) for representative human gallbladder biles. All phase diagrams display the same axes and physical states at equilibrium as in legend to Fig. 1. Symbol ● (left panels) represents the relative lipid compositions of gallbladder biles from Ch gallstone patients in Fig. 3(a–c) and a control bile in Fig. 3(d). Arabic numbers (1 to 7) on curves (right panels) represent the appearance and persistence times of arc, helical, tubular, ChM, small, aggregated, and fused liquid crystals (see ref. 5), respectively. Arrows in the right panels indicate the first appearance of ChM crystals. (See text for further description).

TABLE 2. Bile salt species in gallbladder biles

Bile Salts	Cholesterol Stones	Pigment Stones	Controls
TUDC	1.03 ± 0.43[a,b]	2.52 ± 1.02	2.92 ± 0.57
GUDC	1.87 ± 1.66	2.75 ± 2.29	2.16 ± 0.52
TC	9.19 ± 4.43	7.71 ± 3.51	13.12 ± 3.62
GC	19.30 ± 5.25	24.79 ± 3.99	20.16 ± 0.94
TCDC	9.31 ± 4.66[a]	9.45 ± 4.36[c]	16.25 ± 1.09
GCDC	19.02 ± 3.66[c,d]	34.02 ± 9.74	26.11 ± 5.80
TDC	8.21 ± 3.34[d]	2.65 ± 2.26	4.90 ± 2.02
GDC	26.01 ± 7.87[d,e]	12.07 ± 3.34	10.78 ± 0.56
TLC	0.11 ± 0.26	0.00	0.00
GLC	0.55 ± 0.60[f]	0.41 ± 0.40	0.00
TLCS	1.88 ± 0.78[d]	1.14 ± 0.74	1.91 ± 0.98
GLCS	3.54 ± 2.28	2.50 ± 1.85	1.72 ± 0.39
Total UDC	2.9 ± 1.93	5.27 ± 2.98	5.08 ± 0.71
Total C	28.49 ± 6.76	32.50 ± 3.25	33.28 ± 4.43
Total CDC	28.32 ± 6.48[a,f]	43.47 ± 6.89	42.35 ± 5.90
Total DC	34.22 ± 9.67[a,d]	14.72 ± 5.36	15.67 ± 2.02
Total LC	0.66 ± 0.69[f]	0.41 ± 0.40	0.00
Total LCS	5.41 ± 2.68	3.64 ± 2.47	3.63 ± 0.91
Total DC + LC + LCS	40.29 ± 11.56[a,d]	18.77 ± 7.85	19.30 ± 2.38

[a]Compared with control group $P < 0.0001$.
[b]Compared with pigment stone group $P < 0.05$.
[c]Compared with control group $P < 0.05$.
[d]Compared with pigment stone group $P < 0.01$.
[e]Compared with control group $P < 0.01$.
[f]Compared with pigment stone group $P < 0.0001$.

crystallization. In contrast, most biles that plotted in region ***C*** entered region ***B*** during crystallization (Fig. 1), possibly explaining the more complex liquid crystalline, ChM and putatively anhydrous crystallization sequences. As biles with relative lipid compositions plotting in region ***D*** did not cross phase boundary ***ab*** during crystallization (Fig. 1), sequences did not change. These observations on human biles (Fig. 1) agree precisely with the behavior of model bile systems during crystallization (5). Figure 1 also verifies that the micellar lipid compositions of gallbladder biles from controls and pigment gallstone patients changed little during prolonged incubation at 37°C over that expected by experimental error.

Molecular species of BS in gallbladder biles

Table 2 lists the proportions of 12 common conjugated BS species present in each set of biles. The major differences were the significantly higher proportions of GDC and GLC and lower proportions of TUDC, TCDC, and GCDC in biles from Ch stone patients compared with those from controls and pigment stone patients. Furthermore, the percent secondary BS (DC plus LC and SLC) levels were significantly smaller (18.8% and 19.3%) in pigment stone and control biles respectively, compared with Ch stone biles (40.3%). Curiously, pigment stone biles had a significantly lower TCDC content compared with control biles.

Ch crystallization in gallbladder biles with added EDTA

No calcium bilirubinate precipitates were found in EDTA biles, but amorphous nonbirefringent strands of golden-brown calcium bilirubinate precipitates became apparent in all gallbladder biles without EDTA. Appearance times of calcium bilirubinate were strongly temperature-dependent, occurring within 1 day at 37°C and 45°C, in 2–4 days at 23°C, and 3–6 days at 4°C. Ch crystal and liquid crystal sequences occurred on the same day or ± one day in biles with or without EDTA but no systematic trend was discernible. Total calcium concentration in control and Ch gallstone biles was 5.61 ± 3.98 mM. This value was significantly smaller ($P < 0.05$) than the calcium content of the bile samples (n = 4) from patients with pigment gallstones (12.43 ± 6.87 mM).

DISCUSSION

We have explored whether the crystallization pathways and sequences in human gallbladder biles agreed with the ones observed in model bile systems (5). To achieve this comparison, native biles were separated from ChM crystals and lamellar liquid crystals and were forced to recrystallize. The major findings may be summarized as follows. *i*) Habits of solid Ch crystals and

liquid crystals found in model bile systems (5) were observed in gallbladder biles during crystallization. *ii*) Crystallization sequences in native biles were identical to those in MBS–L–Ch model systems for the appropriate BS/L ratio, [TL], and temperature. *iii*) Sizes of ChM crystals in human Ch gallstone biles were larger (216.8 ± 223.4 μm^2/per ChM plate) than in model biles (84.0 ± 71.4 μm^2/per ChM plate) and in gallbladder biles of male inbred mice during lithogenesis (57.2 ± 64.5 μm^2/per ChM plate) (20–22) and this may possibly be attributable to the higher average CSI (=1.56) and [TL] (=12.1 g/dL) values of human biles compared with mouse biles (CSI = 1.17; [TL] = 7.4 g/dL) and model biles (CSI = 1.19; [TL] = 7.3 g/dL). *iv*) Arc-like crystals that have the buoyant density of anhydrous Ch (5) are a feature of crystallization in human biles, but only in those with relative compositions plotting in pathways ***B*** and ***C*** (Fig. 1), i.e., those with the highest BS to L ratios (1). Even though needle-shaped Ch crystals have been noted previously during crystallization from pure Ch–L vesicle systems (23), and from model (24, 25) and animal biles (26), their pathophysiological importance as an apparently "anhydrous mode" of Ch crystallization was not appreciated until recently (3, 5, 19). One possibility for the failure to document needle- or arc-shaped crystals and the metastable intermediates (helical and tubular crystals) may be because investigators were either unaware of their transient occurrences in human gallbladder biles, or failed to monitor bile samples after the first microscopic appearance of ChM crystals (1). Recently, other investigators (27–29) have confirmed arc-like crystals in model and human biles using video-enhanced and polarizing light microscopy. Tubular crystals are metastable intermediates between arcs and ChM crystals (5, 19) and in the present work they were observed in only two biles prior to ultracentrifugation and microfiltration (Fig. 2). Most relative lipid compositions of Ch gallstone biles plotted in pathways ***B*** and ***C*** (Fig. 1) and therefore ACh appeared after ChM crystals. In inbred mice fed a lithogenic diet, the BS pool becomes predominantly (~70%) taurocholate; therefore arc, filamentous, and tubular crystals are expected and observed (21, 22) in biles plotting in pathway ***B*** (Fig. 1).

Studying temperature-dependence of Ch crystallization provided a method to show how phase boundaries influence Ch crystallization pathways and demonstrated that crystallization sequences may differ despite identical biliary compositions. Even though the dilution of a bile sample could theoretically lead to a similar effect because of a shift in phase boundaries (5), the concentrations of critical nuclei, microcrystals, pro- and anti-crystallizing proteins, etc. would have been diluted and hence the frame of reference for comparison with the undiluted native bile would have been altered. Therefore, temperature-dependence studies of crystallization pathways facilitated new insights into the universality of the model crystallization pathways (5) and showed that protein factors and perhaps other biliary micro-components do not influence the crystal/liquid crystal sequences (5).

Increased levels of DC conjugates in Ch gallstone biles have been noted many times (30–35). Using model bile systems, Stolk et al. (27) showed that more hydrophobic BS induced rapid Ch crystal precipitation, as was also verified in our model bile study (5). Furthermore, using freeze fracture transmission electron microscopy, van de Heijning and colleagues (36) found that hydrophobic BS induced more rapid aggregation and fusion of vesicles in bile to form multilamellar structures, also favoring Ch crystallization (5, 35, 37–39). Insights on the reasons for this may be inferred from our model bile studies (5). An increase in BS hydrophobicity shifts all phase boundaries and crystallization pathways on the phase diagrams to the right. For biles of the same relative lipid compositions, this favors more rapid ChM crystallization as more human biles would tend to plot in pathway ***B*** (Fig. 1) where ChM crystallizes faster.

Some (24, 37, 40) but not all (41, 42) investigators have shown that calcium salts influence Ch crystallization and/or crystal growth in model and native biles. In our model bile study (5) we found that only crystal growth and number but not crystal detection times were accelerated by calcium concentrations >5 mM. During and after gallstone formation (43, 44), an increase in biliary calcium levels often occurs in experimental animals, but the confounding variable is that calcium levels may be related to increased concentration and accumulation of mucin gel in the gallbladder (45). In the experimental strategy used in the present study, we found that chelation of calcium by EDTA did not influence solid and liquid crystal sequences nor appearance times in native bile, confirming that calcium bilirubinate is not a Ch crystallization promoter (10, 42). However, in the present studies, it was not possible to determine whether calcium chelation actually decreased Ch crystal numbers as the total calcium level (mean = 5.6 mM) in Ch gallstone biles would be expected on the basis of our model studies (5) to have an insufficient effect.

In conclusion, the present study reveals that relative lipid compositions of gallbladder biles from Ch gallstone patients fall into three distinct crystallization pathways. These pathways and sequences for a pathophysiological range of lipid compositions were identical to those of appropriately patterned model biles (5). They show putatively anhydrous Ch, ChM crystallization, and liquid crystal precipitation in distinct sequences. Fur-

thermore, physiologic calcium levels did not alter crystallization pathways and sequences, although in model systems 5–20 mM concentrations of the divalent cation promoted Ch crystal growth (5). However, this range fell outside the physiological limits of total calcium found in Ch gallstone biles in the present work. In addition, in ex vivo human biles, insoluble calcium bilirubinates were not a promoter of Ch crystallization or crystal growth. It is anticipated that these studies will provide a more rigorous experimental framework for determination of the pathophysiological and physical–chemical roles of nucleating/crystallizing factors in native bile.

We thank Dr. David C. Brooks, Department of Surgery at Brigham and Women's Hospital, Boston for his generous cooperation in providing samples of human bile and gallstones. We are also grateful to Ms. Monika Leonard who provided outstanding technical and editorial expertise, Miss Elaine O'Rourke for word-processing the manuscript, and Drs. David E. Cohen, Frank Lammert, and Karel J. van Erpecum for their scientific advice. This study was supported in part by grants DK 36588 and DK 34854 from the National Institutes of Health (US Public Health Service).

Manuscript received 19 September 1996.

REFERENCES

1. Holan, K. R., R. T. Holzbach, R. E. Hermann, A. M. Cooperman, and W. J. Claffey. 1979. Nucleation time: a key factor in the pathogenesis of cholesterol gallstone disease. *Gastroenterology.* **77:** 611–617.
2. Carey, M. C. 1993. Pathogenesis of gallstones. *Am. J. Surg.* **165:** 410–419.
3. Konikoff, F. M., D. S. Chung, J. M. Donovan, D. M. Small, and M. C. Carey. 1992. Filamentous, helical, and tubular microstructures during cholesterol crystallization from bile. Evidence that cholesterol does not nucleate classic monohydrate plates. *J. Clin. Invest.* **90:** 1155–1160.
4. Holzbach, R. T., and C. Corbusier. 1978. Liquid crystals and cholesterol nucleation during equilibration in supersaturated bile analogs. *Biochim. Biophys. Acta.* **528:** 436–444.
5. Wang, D. Q.-H., and M. C. Carey. 1996. Complete mapping of crystallization pathways during cholesterol precipitation from model bile: influence of physical–chemical variables of pathophysiologic relevance and identification of a stable liquid crystalline state in cold, dilute, and hydrophilic bile salt-containing systems. *J. Lipid Res.* **37:** 606–630.
6. Harvey, R. C., D. Taylor, C. N. Petrunka, A. D. Murray, and S. M. Strasberg. 1985. Quantitative analysis of major, minor and trace elements in gallbladder bile. *Hepatology.* **5:** 129–132.
7. Moore, E. W. 1984. The role of calcium in the pathogenesis of gallstones: Ca^{++} electrode studies of model bile salt solutions and other biologic systems. *Hepatology.* **4:** 228S–243S.
8. Sutor, D. J., and L. I. Wilkie. 1977. Calcium in bile and calcium salts in gallstones. *Clin. Chim. Acta.* **79:** 119–127.
9. Ostrow, J. D. 1984. The etiology of pigment gallstones. *Hepatology.* **4:** 215S–232S.
10. Gallinger, S., P. R. C. Harvey, C. N. Petrunka, and S. M. Strasberg. 1986. Effect of binding of ionised calcium on the in vitro nucleation of cholesterol and calcium bilirubinate in human gall bladder bile. *Gut.* **27:** 1382–1386.
11. Hotchkiss, R. D. 1948. A microchemical reaction resulting in the staining of polysaccharide structures in fixed tissue preparations. *Arch. Biochem.* **16:** 131–135.
12. Turley, S. D., and J. M. Dietschy. 1978. Re-evaluation of the 3α-hydroxysteroid dehydrogenase assay for total bile acids in bile. *J. Lipid Res.* **19:** 924–928.
13. Bartlett, G. R. 1959. Phosphorus assay in column chromatography. *J. Biol. Chem.* **234:** 466–468.
14. Fromm, H., P. Amin, H. Klein, and I. Kupke. 1980. Use of a simple enzymatic assay for cholesterol analysis in human bile. *J. Lipid Res.* **21:** 259–261.
15. Carey, M. C. 1978. Critical tables for calculating the cholesterol saturation of native bile. *J. Lipid Res.* **19:** 945–955.
16. Goh, E. H., S. M. Colles, and K. D. Otte. 1989. HPLC analysis of desmosterol, 7-dehydrocholesterol, and cholesterol. *Lipids.* **24:** 652–655.
17. Rossi, S. S., J. L. Converse, and A. F. Hofmann. 1987. High pressure liquid chromatographic analysis of conjugated bile acids in human bile: simultaneous resolution of sulfated and unsulfated lithocholyl amidates and the common conjugated bile acids. *J. Lipid Res.* **28:** 589–595.
18. Bowers, G. N., Jr., and T. C. Rains. 1988. Measurement of total calcium in biological fluids: flame atomic absorption spectrometry. *Methods Enzymol.* **158:** 302–319.
19. Chung, D. S., G. B. Benedek, F. M. Konikoff, and J. M. Donovan. 1993. Elastic free energy of anisotropic helical ribbons as metastable intermediates in the crystallization of cholesterol. *Proc. Natl. Acad. Sci. USA.* **90:** 11341–11345.
20. Khanuja, B., Y-C. Cheah, M. Hunt, P. M. Nishina, D. Q-H. Wang, H. W. Chen, J. T. Billheimer, M. C. Carey, and B. Paigen. 1995. *Lith* 1, a major gene affecting cholesterol gallstone formation among inbred strains of mice. *Proc. Natl. Acad. Sci. USA.* **92:** 7729–7733.
21. Wang, D. Q.-H., B. Paigen, and M. C. Carey. 1995. Phenotype characterization of *Lith* genes determining susceptibility to cholesterol gallstone formation in inbred mice. *Hepatology.* **22:** 289A.
22. Wang, D.Q-H., B. Paigen, and M. C. Carey. 1996. Genetic and environmental factors determine cholesterol gallstone incidence in inbred mice. *Gastroenterology.* **110:** A1357.
23. Collins, J. J., and M. C. Phillips. 1982. The stability and structure of cholesterol-rich codispersions of cholesterol and phosphatidylcholine. *J. Lipid Res.* **23:** 291–298.
24. Toor, E. W., D. F. Evans, and E. L. Cussler. 1978. Cholesterol monohydrate growth in model bile solutions. *Proc. Natl. Acad. Sci. USA.* **75:** 6230–6234.
25. Lichtenberg, D., S. Ragimova, A. Bor, S. Almog, C. Vinkler, M. Kalina, Y. Peled, and Z. Halpern. 1988. Stability of mixed micellar bile models supersaturated with cholesterol. *Biophys. J.* **54:** 1013–1025.
26. Jenkins, S. A. 1978. Biliary lipids, bile acids and gallstone formation in hypovitaminotic C guinea pigs. *Br. J. Nutr.* **40:** 317–322.
27. Stolk, M. F. J., B. J. M. van de Heijning, K. J. van Erpecum, A. M. W. C. van den Broek, W. Renooij, and G. P. van Berge-Henegouwen. 1994. The effect of bile acid hydrophobicity on nucleation of several types of cholesterol crystals from model bile vesicles. *J. Hepatol.* **20:** 802–810.
28. Kaplun, A., Y. Talmon, F. M. Konikoff, M. Rubin, A. Eitan,

M. Tadmor, and D. Lichtenberg. 1994. Direct visualization of lipid aggregates in native human bile by light- and cryo-transmission electron-microscopy. *FEBS Lett.* **340:** 78–82.
29. Juste, C., I. Catala, R. Henry, C. Chabanet, A-M. Gueugneau, F. Béguet, B. Lyan, and T. Corring. 1995. Influence of bile salt molecular species on cholesterol crystallization from supersaturated model biles. *Biochim. Biophys. Acta.* **1254:** 89–97.
30. Carey, M. C., and W. C. Duane. 1994. Enterohepatic circulation. *In* The Liver: Biology and Pathobiology. I. M. Arias, J. L. Boyer, N. Fausto, W. B. Jakoby, D. A. Schachter, and D. A. Shafritz, editors. New York, Raven Press, Ltd. 719–767.
31. Low-Beer, T. S., and E. W. Pomare. 1975. Can colonic bacterial metabolites predispose to cholesterol gall stones? *Br. Med. J.* **1:** 438–440.
32. van der Werf, S. D. J., and G. P. van Berge-Henegouwen. 1983. Biliary bile acid composition and cholesterol saturation. *Gastroenterology.* **84:** 1074–1077.
33. Marcus, S. N., and K. W. Heaton. 1986. Intestinal transit, deoxycholic acid and the cholesterol saturation of bile—three inter-related factors. *Gut.* **27:** 550–558.
34. Marcus, S. N., and K. W. Heaton. 1988. Deoxycholic acid and the pathogenesis of gall stones. *Gut.* **29:** 522–533.
35. Hussaini, S. M., S. P. Pereira, G. M. Murphy, and R. H. Dowling. 1995. Deoxycholic acid influences cholesterol solubilization and microcrystal nucleation time in gallbladder bile. *Hepatology.* **22:** 1735–1744.
36. van de Heijning, B. J. M., M. F. J. Stolk, K. J. van Erpecum, W. Renooij, and G. P. van Berge-Henegouwen. 1994. The effects of bile salt hydrophobicity on model bile vesicle morphology. *Biochim. Biophys. Acta.* **1212:** 203–210.
37. Kibe, A., M. A. Dudley, Z. Halpern, M. P. Lynn, A. C. Breuer, and R. T. Holzbach. 1985. Factors affecting cholesterol monohydrate crystal nucleation time in model systems of supersaturated bile. *J. Lipid Res.* **26:** 1102–1111.
38. Halpern, Z., M. A. Dudley, M. P. Lynn, J. M. Nader, A. C. Breuer, and R. T. Holzbach. 1986. Vesicle aggregation in model systems of supersaturated bile: relation to crystal nucleation and lipid composition of the vesicular phase. *J. Lipid Res.* **27:** 295–306.
39. Halpern, Z., M. A. Dudley, A. Kibe, M. P. Lynn, A. C. Breuer, and R. T. Holzbach. 1986. Rapid vesicle formation and aggregation in abnormal human biles. A time-lapse video-enhanced contrast microscopy study. *Gastroenterology.* **90:** 875–885.
40. Berenson, M. M., and J. R. Cardinal. 1985. Calcium accelerates cholesterol phase transitions in analog bile. *Experientia.* **41:** 1328–1330.
41. Neithercut, W. D. 1989. Effect of calcium, magnesium, and sodium ions on in vitro nucleation of human gall bladder bile. *Gut.* **30:** 665–670.
42. Whiting, M. J., and J. McK. Watts. 1985. Cholesterol gallstone pathogenesis: a study of potential nucleating agents for cholesterol crystal formation in bile. *Clin. Sci.* **68:** 589–596.
43. Shiffman, M. L., H. J. Sugerman, J. M. Kellum, and E. W. Moore. 1992. Calcium in human gallbladder bile. *J. Lab. Clin. Med.* **120:** 875–884.
44. Rudnicki, M., T. Jørgensen, and J. Thode. 1992. Increased activity of ionised calcium in gall bladder bile in gall stone disease. *Gut.* **33:** 1404–1407.
45. LaMont, J. T., and M. C. Carey. 1992. Cholesterol gallstone formation. 2. Pathobiology and pathomechanics. *Prog. Liver Dis.* **10:** 165–191.